Band structure of indium selenide investigated by intrinsic photoluminescence under high pressure

F. J. Manjón,[1,2,*] A. Segura,[1] V. Muñoz-Sanjosé,[1] G. Tobías,[3] P. Ordejón,[3] and E. Canadell[3]
[1]*Departament de Física Aplicada i Institut de Ciència dels Materials de la Universitat de València, C/. Dr. Moliner, 50, 46100 Burjassot, València, Spain*
[2]*Departament de Física Aplicada, Universitat Politècnica de València, E.P.S.A. 03801 Alcoi, Alacant, Spain*
[3]*Institut de Ciència dels Materials de Barcelona, CSIC, Campus de la UAB, 08193 Bellaterra, Barcelona, Spain*
(Received 8 April 2004; revised manuscript received 26 May 2004; published 1 September 2004)

This paper reports on photoluminescence experiments in *n*-type indium selenide ($T=300$ K) under hydrostatic pressure up to 7 GPa at low and high excitation densities. Photoluminescence measurements at low excitation density exhibit a broad band around the energy of the direct band gap of InSe and with the same pressure dependence. The reversible increase of its linewidth above 1 GPa is associated to a direct-to-indirect band-gap crossover between valence band maxima. The reversible decrease of its intensity above 4 GPa is interpreted as evidence of a direct-to-indirect band-gap crossover between conduction band minima. Photoluminescence measurements under high excitation density exhibit several spontaneous and stimulated emission bands. The different components of these bands can be attributed to radiative emission from different minima of the conduction band to different maxima of the valence band in the framework of the band-gap renormalization theory in a multivalley scenario. The image of the electronic band structure of InSe provided by these measurements agrees with the previous analysis of the optical absorption coefficient of InSe and $In_{1-x}Ga_xSe$.

DOI: 10.1103/PhysRevB.70.125201 PACS number(s): 71.20.Nr, 71.35.Ee, 78.45.+h, 78.47.+p

I. INTRODUCTION

Layered III–VI semiconductor compounds have long been studied due to the unusual nature of electronic interactions present in such compounds, and also due to their potential application in nonlinear optics,[1–5] solar cells,[6] memory devices,[7] and solid state batteries.[8] Recently, III–VI layered materials are the object of renewed interest due to new applications aroused with van der Waals epitaxy,[9–11] like GaAs surface passivation,[12,13] and the capacity of layered structures to accommodate strong lattice mismatches in order to achieve a good epitaxy of three-dimensional semiconductors.

Extrinsic and intrinsic photoluminescence (PL) measurements in III–VI layered semiconductors have been reported in a number of papers where the high anisotropy and nonlinear properties of these semiconductors have been stressed.[14,15] In particular, gain and stimulated emission measurements in these materials have been performed by different authors and several hypotheses have been argued to explain the nature of the stimulated emissions at room and low temperatures.[16–30] Many of these studies (performed during the latest 40 years) failed in correlating the unusual electronic properties of these compounds and the electronic band structure obtained from theoretical calculations. The main reason for the failure was the lack of detailed knowledge of the electronic band structure near the fundamental band gap.

Some theoretical band structure calculations of InSe were not appropriate for the comparison with experiments done on the γ polytype. The reason was either because of the assumption of a different polytype (ε or β), far much simpler for calculations, or because of the calculation of the band structure in directions of the Brillouin zone (e.g., Γ-*A* or Γ-*B*) hardly accessible by experimental methods. In the last decade, modern theoretical calculations have succeeded in the description of the band structure of III–VI compounds, specially the γ-polytype InSe and the monoclinic GaTe, which are the more complex III–VI layered semiconductors.[31–38] Figure 1 shows the Brillouin zone of the γ-polytype InSe, which belongs to the rhombohedral space group $C_{3v}^5(R3m)$. These semiconductors have a direct gap at the *Z* point of the Brillouin zone at ambient pressure and become indirect semiconductors with increasing pressure. In the case of InSe, two direct-to-indirect crossovers were observed in absorption measurements under pressure.[34,36] These results were interpreted on the basis of numeric-atomic-orbital-density-functional-theory (NAO-DFT) band structure calculations. Figure 2(a) shows a scheme of the calculated band structure of InSe near the fundamental band gap at different pressures.[34,36] The two indirect transitions observed under pressure in optical measurements were assigned to transitions I_1 and I_2 in Fig. 2(a). Transition I_1 occurs from a shoulder near the valence band maximum (VBM) at *Z* that develops into a new VBM above 1.2 GPa. Transition I_2 occurs from the VBM at *Z* to the *B* conduction band minima (CBM), that becomes the absolute minima around 4 GPa.

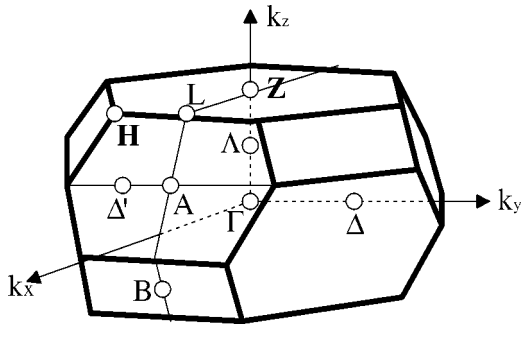

FIG. 1. Rhombohedral Brillouin zone of γ-InSe.

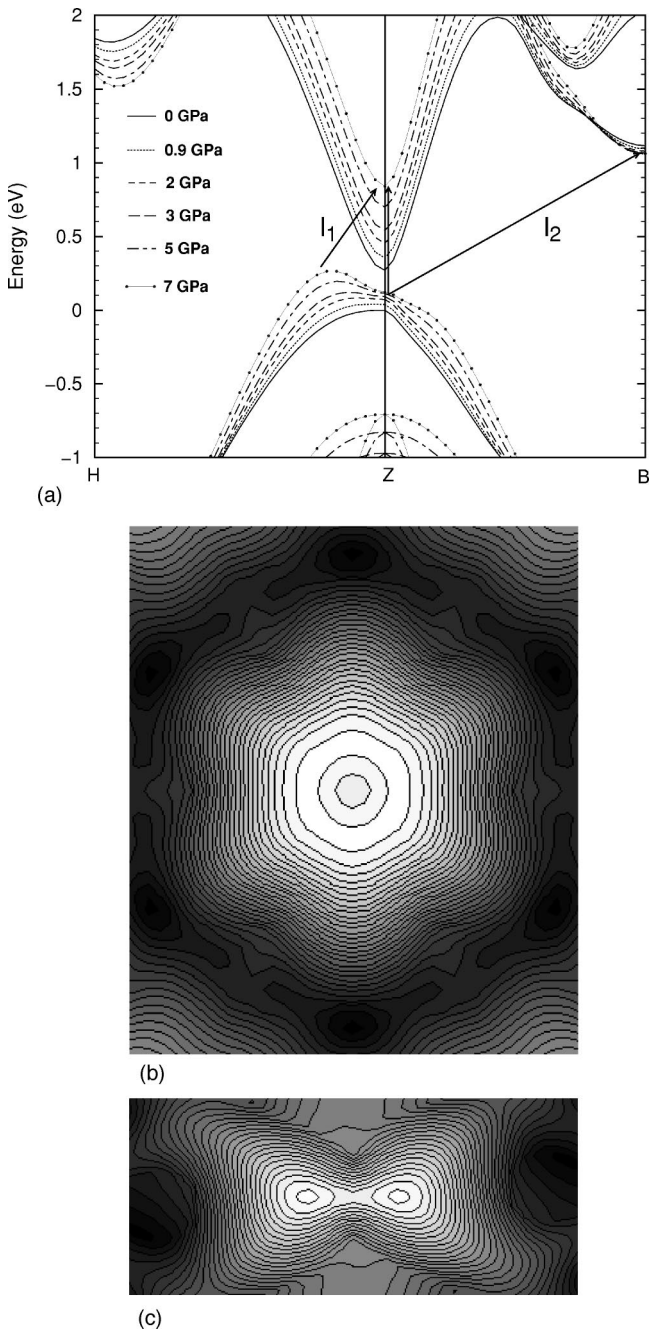

FIG. 2. (a) Scheme of the band structure of InSe near the fundamental Z direct band gap at different pressures according to NAO-DFT band structure calculations. A shoulder in the valence band appears with increasing pressure. The shoulder has thoroidal (donut) symmetry around the Z point, as shown by the top and lateral views of the cross sections of the constant energy surfaces shown in (b) and (c), respectively. Clearer gray colors correspond to higher energy. The shoulder is responsible for the I_1–Z indirect transition at high pressure. The B minima of the conduction band decrease in energy with increasing pressure and is responsible for the Z–I_2 indirect transition at high pressure.

Recent quasi-particle GW calculations suggest that the conduction band crossover occurs between the Z and A CBM.[37] In the following we assume that the direct-to-indirect crossover of the conduction bands is between the Z and B minima. Figures 2(b) and 2(c) show that the pressure-induced VBM has a quasi-cylindrical symmetry with center at the Z point. This symmetry corresponds to thoroidal shape constant energy surfaces that give rise to a 2D-like density of states.[36]

In this paper, we present a study of the PL of InSe at room pressure as a function of excitation density and we report the pressure dependence of the intrinsic PL in indium selenide in the low- and high-density excitation regime. We interpret the emission bands observed in low-density photoluminescence (LDPL) and the emission bands observed in high-density photoluminescence (HDPL) on the light of the most recent theoretical calculations and on the light of the band-gap renormalization theory (BGR) in a multivalley scenario (BGRMS), that was developed for III–V materials.[39,40] We will demonstrate that the present measurements and the recently calculated electronic band structure of InSe agree with the previously reported analysis of the optical absorption coefficient in InSe and $In_{1-x}Ga_xSe$ ($x<0.2$).[34] Preliminary results of this work have been published in Refs. 41 and 42.

II. EXPERIMENTAL DETAILS

γ-InSe single crystals were grown by the Bridgman–Stockbarger method from a $In_{1.05}Se_{0.95}$ melt.[43] Samples of 10–50 μm in thickness were cleaved perpendicular to the [001] direction from the ingot and contained an electron concentration of 3×10^{16} cm^{-3}, as measured by Hall effect in van der Pauw configuration. Samples showed an intense band-to-band recombination peak at room temperature ensuring a good crystal quality. For measurements under pressure, samples were cut into pieces of 100×100 μm^2 in size and placed together with a ruby chip into a 200 μm diameter hole drilled on a 60 μm thick Inconel gasket and inserted between the diamonds of a membrane-type diamond anvil cell (MDAC).[44]. A 4:1 methanol–ethanol mixture was used as pressure-transmitting medium ensuring hydrostatic conditions up to 10 GPa.[45] Pressure was determined by the shift of the ruby PL lines[46] with a spectral resolution of 0.5 Å. PL signal was dispersed by a 1 m single-grating monochromator with a spectral resolution of 16 Å/mm in the slit plane.

A. Low-density photoluminescence measurements

Room-temperature LDPL measurements as a function of pressure were carried out both in the transmission and reflection configuration by exciting samples with a HeNe laser (632 nm). The laser beam was chopped at low frequency and focused in the sample inside the DAC using a microscopic objective. The excited portion of the sample was a 30-μm-diameter spot of the central region of the sample. A spatial filtering system, consisting of a 20× microscope objective and a pinhole, was used to select LDPL signal coming from a 25-μm-diameter spot of the excited region of the sample. The LDPL signal was then analyzed with a 1-m-focal length monochromator, detected by a Si photodiode and registered synchronously with a lock-in amplifier. The spectral bandwidth was set to 16 Å for LDPL measurements.

B. High-density photoluminescence measurements

Room-temperature PL measurements as a function of the excitation density and HDPL measurements as a function of pressure (at a constant excitation density) were taken using the transmission configuration. The whole sample was excited with pulses generated by a frequency-doubled Nd:YAG laser with 532 nm, 7 ns FWHM, and 10 Hz repetition rate. In order to avoid sample damaging no focusing lenses were used. The same spatial filtering system previously described was used to select HDPL signal coming from a 25-μm-diameter spot of the excited central region of the sample. The HDPL signal was detected by an ultrafast Si photodiode and a boxcar system synchronized with the repetition frequency of the laser. The spectral bandwidth was set to 50 Å for HDPL measurements.

Typical excitation powers of 10–12 mW, giving a fluency about 3.5 mJ/cm^2 or equivalently a photon flux of 10^{24} cm^{-2} s^{-1} were used. As the absorption coefficient of InSe at 532 nm is 1.2×10^4 cm^{-1},[47] the penetration depth of the laser pulse is around 1 μm. With these data, we estimate an electron-hole generation rate of 1.2×10^{28} cm^{-3} s^{-1} and assuming a carrier lifetime of 10 ns,[4,5] we get a density of photoexcited carriers of about 1.2×10^{20} cm^{-3}. An average temperature increase of 10 K has been measured under these excitation conditions outside the DAC[4] so a lower overall heating of the sample inside the DAC is expected because of the thermal contact with the pressure transmitting medium.

III. RESULTS AND DISCUSSION

A. Measurements at low-excitation density

Figure 3(a) shows the pressure evolution of LDPL spectra of InSe at room temperature up to 5.6 GPa in the transmission configuration. The LDPL spectra consist of two bands of different intensity and similar behavior under pressure. Spectra taken at the reflection configuration are similar to those of Fig. 3(a) but with a smaller relative intensity of the low energy peak. Figure 3(b) shows the two-component fit of one of those spectra. The high-energy band is close to the direct band-gap energy of InSe. We have modeled this band to the usual expression of band-to-band (BB) PL direct edge transition.

$$I_{\mathrm{BB}}(\hbar\omega) = \int_{E_0}^{\infty} C\sqrt{\hbar\omega' - E_0}\exp\left(-\frac{\hbar\omega' - E_0}{kT}\right) \times\exp\left[-\frac{1}{2}\left(\frac{\hbar\omega - \hbar\omega'}{\sigma}\right)^2\right]d\hbar\omega'. \qquad (1)$$

The Gaussian convolution function is used in order to take into account the scattering mechanisms widening the electronic transitions. Equation (1) has been fitted to BB spectra at different pressures with four free parameters (C, E_0, T, and σ). Let us note that temperature, as obtained from the fits, stays almost constant (about 350 K) at different pressures. This temperature increase is a consequence of the local heating of the sample under absorption of the whole laser intensity. On the other hand, the low-energy band has been modeled with a Gaussian centered at a photon energy E_0'. Figure 4 shows that the pressure dependence of E_0 and E_0' is nearly the same as that of the direct gap in InSe.[33,34] Furthermore, both bands show the same pressure dependence of the intensity and FWHM. This result supports the assignment of both bands to the direct band-to-band transition. We assign the weak band to the modification of the internal PL spectrum as a result of reabsorption, nonhomogenous excitation and local heating of the sample by the excitation laser. Such hypothesis is supported by the smaller intensity of the low-energy band in the reflection configuration.

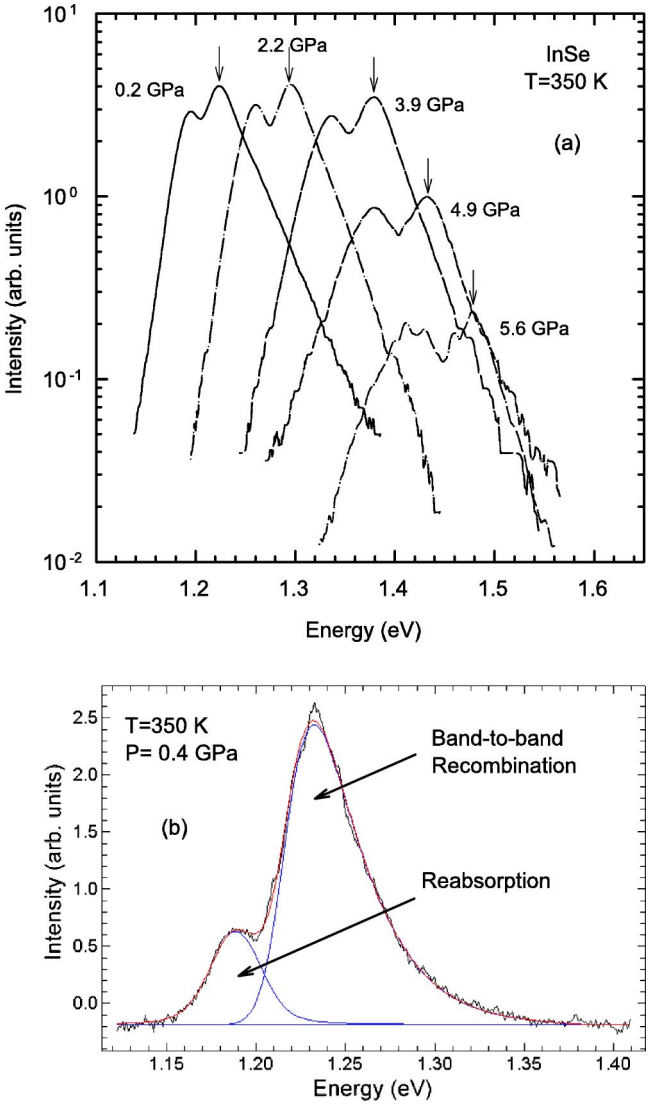

FIG. 3. (a) Room-temperature PL spectra of InSe at different pressures under low excitation conditions in the transmission configuration. (Color online) (b) Room-temperature PL spectrum of InSe in the reflection configuration at $P=0.4$ GPa showing the decomposition of the spectra. The BB recombination has been modeled with a square-root function convoluted by a Gaussian [Eq. (1)], and the reabsorption of the sample with a Gaussian profile.

The inset of Fig. 4 shows the pressure evolution of the convolution Gaussian width σ. A reversible increase of σ is observed above 1.2 GPa. We attribute such increase to the onset of a new carrier scattering process above that pressure. A similar increase of the exciton linewidth above 1–1.5 GPa

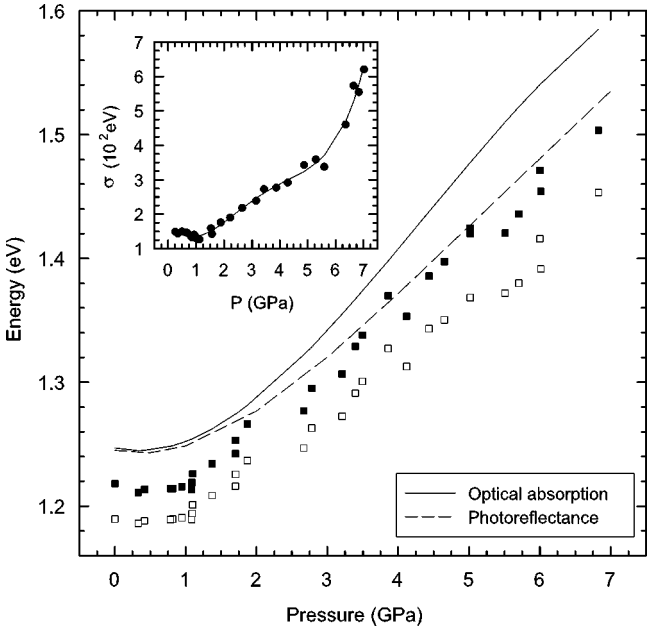

FIG. 4. Pressure dependence of the energy of the band gap, as obtained from the fit of the BB emission (filled symbols), and of the energy of the maximum of the reabsorption band (hollow symbols) in InSe at room temperature. The pressure dependence of the band-gap energy obtained from absorption (solid line) and photoreflectance (dotted line) are shown for comparison. The inset shows the pressure dependence of the width of the convoluting Gaussian of the square root function corresponding to the Maxwell–Boltzmann edge.

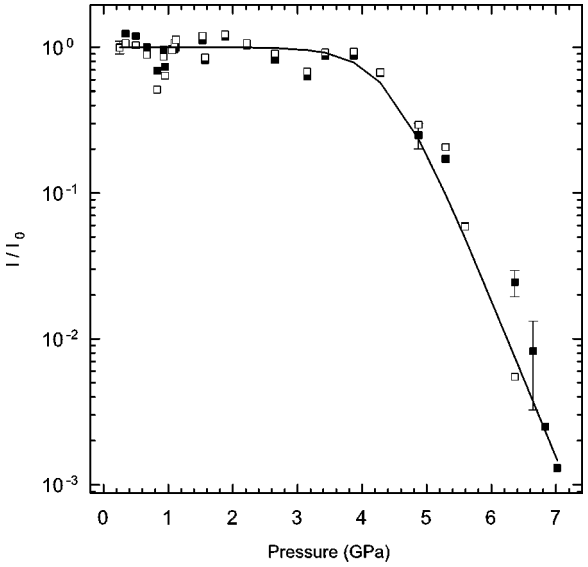

FIG. 5. Pressure dependence of the relative intensity of the BB emission (filled symbols) and of the reabsorption band (hollow symbols). The solid line represents the pressure dependence of the intensity modeled with Eq. (5).

was observed in optical absorption measurements in InSe at low[48] and room temperature.[34] This behavior was attributed to the evolution of the valence band structure under pressure[34] (see Fig. 2). The thoroidal VBM around Z shifts to higher energies with a larger pressure coefficient than the VBM at Z, leading to the direct-to-indirect exciton crossover at 1.2 GPa. The crossover results in a strong widening of both the direct exciton (as observed in absorption experiments) and of the BB emission band.

Figure 5 shows the intensity of the BB band as a function of pressure. A correction factor has been introduced in order to take into account the change of the carrier density photogeneration rate due to the decrease of the absorption coefficient at the laser wavelenght (632 nm) with increasing pressure. The intensity of the BB emission remains nearly constant at low pressure and decreases exponentially above 4 GPa in a *fully reversible* way. It seems reasonable to consider the reversible decrease of the BB PL intensity above 4 GPa as a new evidence of the $Z-I_2$ direct-to-indirect band-gap crossover of the conduction band minima (see Fig. 2).

The linear dependence of the intensity of the BB PL band with the excitation density in the range of excitation here studied indicates that it corresponds to radiative recombinations of completely thermalized electrons. In such conditions, the BB PL intensity, I, at thermal equilibrium is proportional to the photoexcited electron concentration in the conduction band minimum at the Z point of the Brillouin zone and the pressure behaviour of the BB PL intensity can be quantitatively accounted for by a simple model. The distribution of photoexcited electrons Δn_i among the Z and B conduction band minima is given by:

$$\frac{\Delta n_B}{\Delta n_Z} = M_B\left(\frac{m_B^*}{m_Z^*}\right)^{3/2}\exp\left(-\frac{\Delta E_{BZ}-\beta_{BZ}P}{kT}\right), \qquad (2)$$

where m_B^* is the density of states effective mass of the B minimum, M_B is the number of equivalent minima of type B of the conduction band, ΔE_{BZ} is the energy difference at ambient pressure between the B minima and the Z minimum of the conduction band, and β_{BZ} is the pressure coefficient of ΔE_{BZ}.

The kinetic equation controlling the recombination process of photoexcited electrons at the i minimum of the conduction band, under assumption of a monomolecular recombination, is given by

$$\frac{d\Delta n_i}{dt} = G_i - \frac{\Delta n_i}{\tau_{ri}} - \frac{\Delta n_i}{\tau_{nri}} = G_i - \frac{\Delta n_i}{\tau_i}, \qquad (3)$$

where G_i, τ_{ri}, and τ_{nri} are the electron generation rate, and the radiative and nonradiative recombination lifetimes at each minimum. The carrier recombination by collision between electrons in different bands has been neglected in the model.[49] In the stationary case at thermal equilibrium, the generation and recombination rates are equal for both Z and B minima and can be combined in the following equation

$$\sum_i R_i = \frac{\Delta n_Z}{\tau_Z} + \frac{\Delta n_B}{\tau_B} = G = \alpha\phi_0, \qquad (4)$$

where R_i is the recombination rate at each i minimum, $G = G_Z + G_B$ is the total generation rate (that it is assumed to be independent of pressure), ϕ_0 is the total photon flux of the

exciting laser, and α is the absorption coefficient at the laser wavelength.

With these hypotheses, and taking into account the multivalley scheme of the conduction band and its pressure dependence,[34] we can obtain an expression for the intensity of the direct band-to-band recombination transition ($I \propto \Delta n_Z/\tau_{rZ}$) as a function of pressure from Eqs. (2) and (4):

$$I(P) = \alpha\phi_0\left(\frac{\tau_Z}{\tau_{rZ}}\right)\left[1 + M_B\frac{\tau_Z}{\tau_B}\left(\frac{m_B^*}{m_Z^*}\right)^{3/2} \times \exp\left(-\frac{\Delta E_{BZ} - \beta_{BZ}P}{kT}\right)\right]^{-1}. \quad (5)$$

Equation (5) gives a quantitative account of the decay of the direct BB emission as function of pressure as due to the thermalization of photoexcited electrons to the upper B minima of the conduction band as they approach the direct minimum at Z with increasing pressure. The fact that no PL of indirect character has been observed above 4 GPa indicates that the nonradiative recombination predominates at the B minima. This can be attributed to the presence of an electron trap associated to the B minima that becomes deeper as pressure increases. The existence of this trap and its pressure dependence was deduced from transport measurements under pressure.[50]

A reasonable fit to the pressure dependence of the BB emission intensity can be obtained with Eq. (5) by assuming as known parameters $\Delta E_{BZ}=0.3$ eV, $T=350$ K, $M_B=3$, $\beta_{BZ}=0.076$ eV/GPa,[34] and using the preexponential factor in Eq. (5) as a fitting parameter. This fit yields the following preexponential factor

$$\frac{\tau_Z}{\tau_B}\left(\frac{m_B^*}{m_Z^*}\right)^{3/2} = 0.8 \pm 0.3 \quad (6)$$

and is shown in Fig. 5 as a solid line. As the effective mass ratio (m_B^*/m_Z^*) is expected to be much larger that unity,[33,34,37] this result simply indicates that $\tau_Z \ll \tau_B$, which is in agreement with the observation of direct BB PL at Z up to a very high pressure.

B. Measurements at high-excitation density

1. Photoluminescence as a function of excited photocarrier density

Figure 6 shows the room-pressure PL spectra of InSe at different excitation densities. Two bands can be observed in such spectra. The broad band, centered around 1.25 eV, exhibits a bandshape almost independent of the excitation density, whereas the intensity shows a linear dependence on the excitation density. We assign this band to direct band-to-band spontaneous emission from the lowest excited regions of the sample. Note that the laser intensity decreases exponentially with the penetration length and the high-density conditions are only satisfied in a region of less than 1 μm thick near the irradiated surface of the sample.

The narrow band, located around 1.18 eV, exhibits a bandshape strongly dependent on the excitation density. The

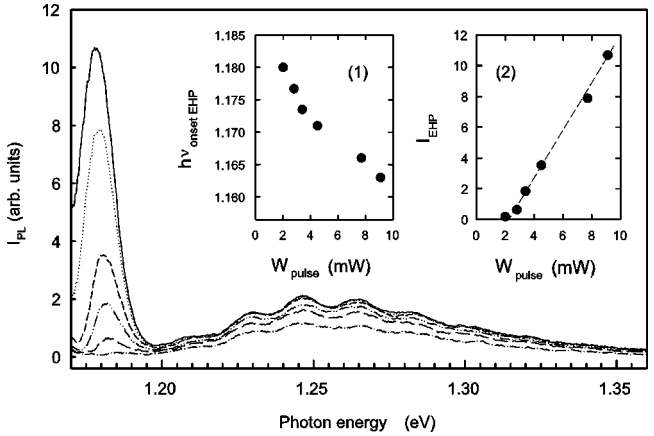

FIG. 6. Room-temperature PL spectra of InSe at different excitation powers (2, 2.8, 3.3, 4.4, 7.7, and 9.2 mW). A low-energy band (DEHP) and a high-energy band (BB) are observed for the highest excitation powers. Inset 1: Evolution of the onset energy of the low-energy tail of the DEHP band as a function of the excitation power. Inset 2: Evolution of the intensity of the DEHP band as a function of the excitation power.

nonlinear redshift of its low energy tail (onset energy) as a function of the excitation density is shown in the inset 1 of Fig. 6. The inset 2 of Fig. 6 shows the linear dependence of the intensity on the excitation density above the threshold power of 2 mW. We assign this band to stimulated emission caused by direct band-to-band recombination of electrons and holes in an electron-hole plasma (DEHP) at high excitation densities on the basis of the existence of a threshold density and of the low-energy tail redshift with increasing density. Our assignment is supported by time-resolved PL measurements measured by us that show a very fast response of the 1.18 eV band (it basically follows the laser pulses) while the 1.25 eV band decays with a much longer lifetime of the order of 9.5 ± 0.5 ns. Let us point out that, as expected in high excitation conditions, recombination is quadratic and the time decay of the broad band exhibits the typical $(1+\beta\Delta n_0 t)^{-1}$ dependence. The value of 9.5 ns corresponds to the instantaneous lifetime at $t=0$ (the product of the quadratic recombination coefficient, β, by the electron concentration at $t=0$, Δn_0).

It is well known that the formation of the degenerate electron-hole plasma (EHP) induces a band-gap renormalization (BGR) in the semiconductor due to the Coulombian interaction between electrons and holes.[39,40,51] The band-gap renormalization can be measured from the difference between the semiconductor band-gap and the onset energy of the EHP stimulated emission band. On the other side, the width of the EHP band allows to calculate the quasi-Fermi levels of electrons (holes), $\mu_e(\mu_h)$, measured from the bottom (top) of the conduction (valence) band, $\Delta\hbar\omega_{\mathrm{EHP}} = \mu_e + \mu_h = (E_{\mathrm{Fe}}^* - E_c) + (E_v - E_{\mathrm{Fh}}^*)$. The total electron and hole densities can be estimated once the quasi-Fermi levels of electrons and holes are known. Finally, the band-gap renormalization at high excitation densities can be calculated with the Vashista–Kalia universal formula.[52]

Figure 7 shows the averaged measured values (symbols) of the Z direct band-gap renormalization in InSe as a func-

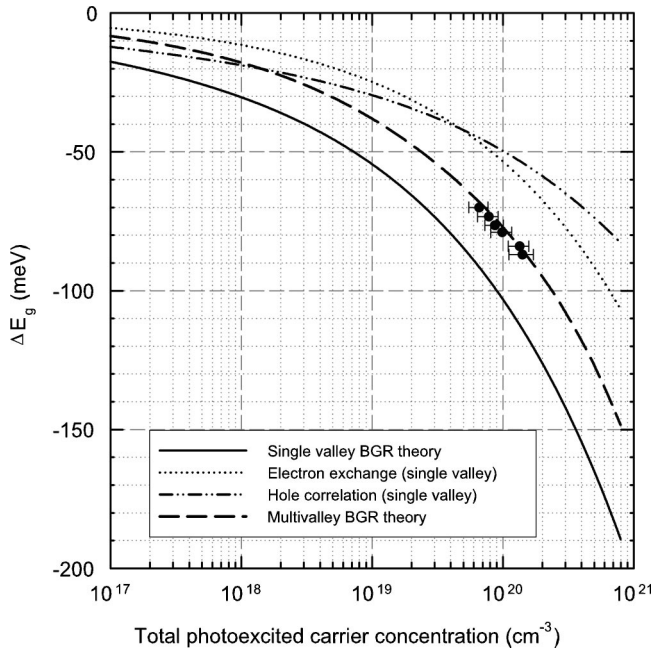

FIG. 7. Experimental estimation of the direct band-gap renormalization in InSe at ambient pressure as a function of the total photoexcited carrier concentration, considering an average diameter light spot of 5.5 mm^2 (symbols). Theoretical estimation of the direct band-gap renormalization energy in InSe in the framework of the BGR theory (solid line) is also shown for comparison. Dotted line corresponds to the correlation energy of electrons and holes plus the electron exchange energy contribution to the direct band-gap renormalization. Dashed-dotted line corresponds to the hole exchange energy contribution if all holes were thermalized in the VBM at *Z*. Dashed line corresponds to the direct band-gap renormalization energy in the framework of the BGRMS theory.

tion of the total photoexcited carrier concentration. The measured values can be compared to the band-gap renormalization energies calculated using the single valley Vashista–Kalia universal formula assuming that all the electrons and holes are thermalized to the VBM and CBM at *Z* (solid line). The calculated renormalization on the above assumption overestimates the measured one, thus suggesting that holes are likely distributed between the *Z* and donut-shaped VBM (see Fig. 2). In fact, the hole concentration in the VBM at *Z*, as estimated from the width of the stimulated emission band (50–70 meV), cannot be higher than 10^{19} cm^{-3}. However, the total excitation hole concentration is as high as 10^{20} cm^{-3} as estimated from the experimental values in Fig. 7. These difficulties can be overcome if we assume that holes are distributed between the *Z* and the donut-like VBM in a multivalley scenario.[39,40]

According to the BGRMS theory,[39,40] the direct gap at *Z* and the indirect gap (between the donut-like VBM and the CBM at *Z*) should have different contributions of the hole exchange interaction to the renormalized band-gap energy. However, both gaps have the same contribution of the correlation energy of electrons and holes and of the electron exchange interaction (because all electrons are basically thermalized to the *Z* minimum of the conduction band). With these considerations, we have plotted in Fig. 7 the correlation energy of electrons and holes plus the total electron exchange energy (dotted line) by subtracting to the total renormalization energy in the single valley scenario (solid line) the total exchange interaction energy of the holes (dashed–dotted line) given by the formula

$$E_{ex} = \frac{-0.916\phi(\rho_h)}{r_s \nu_h^{1/3}}, \tag{7}$$

where r_s is the normalized interparticle distance (calculated assuming an excitonic Rydberg in InSe of 11.7 meV), ν_h is the degeneracy factor of the maximum of the valence band, and ϕ is a function that describes the mass anisotropy in the maximum of the valence band as a function of the ratio of the transverse and longitudinal masses of the holes, ρ_h.[53]

In order to get the correct renormalization energy of the direct band gap we must add the exchange interaction energy of the holes thermalized at the VBM at *Z* to the correlation energy of electrons and holes plus the total electron exchange energy. The exchange interaction energy of the holes thermalized at the VBM at *Z* can be calculated once the hole concentration of the VBM at *Z* is known. The hole concentration in each VBM is given by the Fermi function, the density of states in each valley, and the relative energy position of the different VBM. This relative position is, however, a direct function of the density-induced renormalization of each maximum, so the calculation of the renormalization and population of each maximum of the valence band requires a self-consistent treatment.

In order to calculate the renormalization energy and the population of the VBM at *Z* and at the donut-like VBM at ambient pressure in a self-consistent way, we have taken into account the hole effective mass in the VBM at *Z* ($m_{h\perp} = 0.72m_0, m_{h//} = 0.17m_0$),[54] the excitonic Rydberg in InSe (11.7 meV), and the relative energy position of the two maxima in absence of excitation (70 meV). Furthermore, we have assumed that the donut-like maximum has a density of states given by[36]

$$N_{\text{donut}} = \frac{M_{hd}^* k_0}{\pi\hbar}, \tag{8}$$

where M_{hd}^* is the hole effective mass at the donut, that we have assumed to be around 0.5 m_0, and k_0 is the radius of the donut in the space of quasimomenta around the *Z* point, that according to band structure calculations amounts to 1.5×10^9 m^{-1}.[36] In Fig. 8 we have plotted the distribution of the hole concentration among the two VBM as well as the hole exchange interaction energy of each maxima as a function of the total excitation density at ambient pressure on the above assumptions. This procedure can be done at any pressure to obtain the hole concentration at each VBM and the contribution of the holes to the total renormalization of the bandgap at any pressure, as will be commented later on.

Finally, adding the exchange interaction energy of the holes thermalized in the VBM at *Z* and the correlation energy of electrons and holes plus the total electron exchange energy at ambient pressure, we obtain the total direct band-gap renormalization energy at ambient pressure as a function of

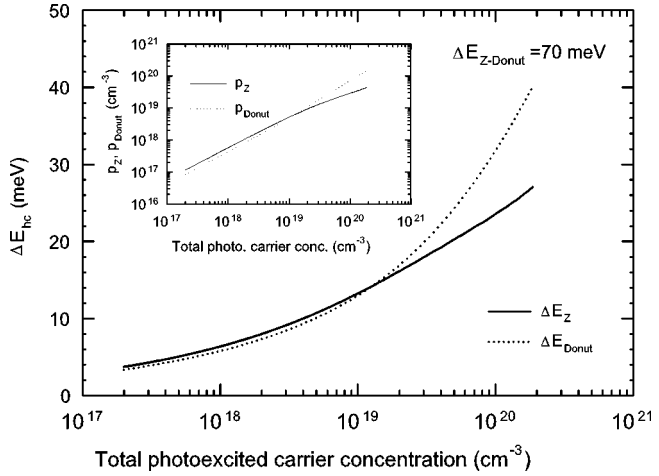

FIG. 8. Hole exchange energy contribution to the renormalization of the direct band gap at Z (solid line) and the I_1-Z indirect band-gap (dotted line) in InSe at ambient pressure as a function of the total photoexcited carrier concentration. Inset shows the hole concentration in the Z and donut-like maxima of the valence band at ambient pressure as a function of the total photoexcited carrier concentration.

the total photoexcited carrier concentration (dashed line in Fig. 7). The calculated renormalization energy of the direct band-gap at ambient pressure in the multivalley scenario agrees nicely with the measured one.

In summary, we have interpreted our results on the PL at ambient pressure as a function of the excitation density from the point of view that a subsidiary donut-like maximum of the valence band is near the absolute maximum at the Z point of the Brillouin zone. We have to note that a similar model was proposed by Godzaev and Sernelius[16] from low-temperature PL measurements as a function of the excitation density. These authors also invoked the closeness of an indirect gap near the direct one at ambient pressure, but they assigned the indirect gap to a transition between the VBM at Z and the CBM at the M point of the Brillouin zone. This assignment is not supported by any of the recent electronic band structure calculations.

2. HDPL as a function of pressure

Figure 9 shows HDPL measurements in InSe (300 K) for a constant excitation density at different pressures up to 5 GPa. Under these conditions, the maximum of the stimulated emission line shifts nonlinearly towards high energies as the direct gap in InSe. The stimulated emission band of the high density-induced EHP is observed up to 5.1 GPa but it is not observed at higher pressures. Let us note that in our measurements despite using an optical filter, the first harmonic of the Nd:YAG laser was not completely removed (1064 nm≈1.165 eV), as observed in Figs. 9–11. We should also note that the excitation conditions of the sample inside the DAC are quite inhomogeneous because of the reflection of the laser pulse on the lateral facets of the diamond.[55]

Figures 10(a) and 10(b) show the HDPL spectra normalized to the height of the stimulated band in two different pressure ranges. The spectra have been shifted to the same

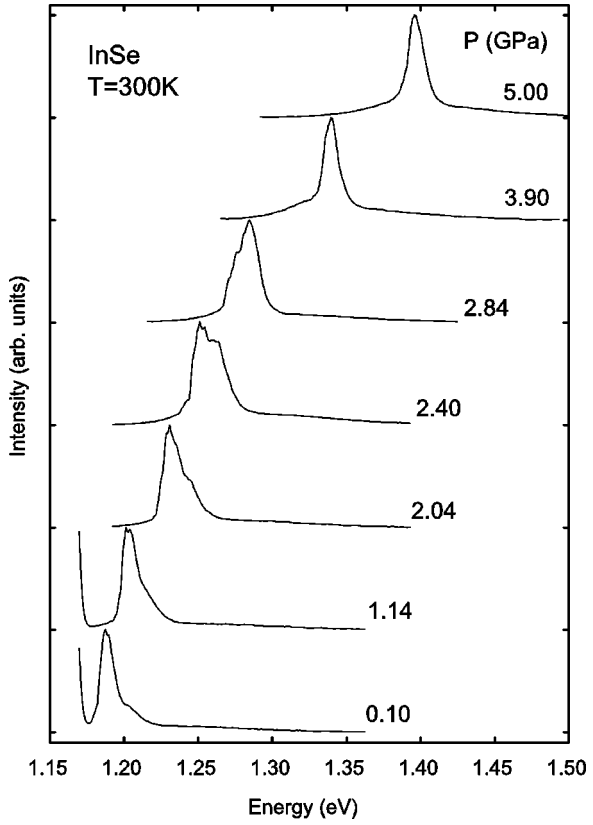

FIG. 9. Room-temperature HDPL spectra of InSe at different pressures under the same high-density excitation conditions. Spectra have been normalized to unity and shifted for the sake of clarity. The low-energy increase appearing in the first spectra corresponds to the first harmonic of the Nd:YAG laser (1064 nm≈1.165 eV) which was not completely removed despite using an optical filter. The stimulated emission peak is no longer seen above 5 GPa.

energy (that of the DEHP peak at ambient pressure) in order to better compare the relative shift of the different components of the spectra as a function of pressure. In Fig. 10(a), HDPL spectra up to 1.7 GPa show a broadening of the high-energy tail of the stimulated DEHP band as pressure increases. The high-energy tail broadening contrasts with the unchanged profile of the low-energy tail of this band in this pressure range. In fact, a low-energy band beginning at 1.15 eV at 1.7 GPa and shifting at the same rate as the stimulated band could be observed in Fig. 10(a) as the emission band shifts to higher energies with respect to the laser line. In this pressure range, we observed only a small increase of the broad BB emission band intensity as compared to that of the stimulated DEHP band.

Figure 10(b) shows how the spectra change drastically above 1.7 GPa. The high energy tail of the stimulated DEHP band broadens up to 2.4 GPa and becomes narrower above such pressure. The low-energy tail broadens considerably and a new low-energy tail appears in the spectra. This new tail shows a different low-energy slope and shifts in energy with a smaller positive pressure coefficient than that of the stimulated DEHP band. The inset of Fig. 10(a) shows the evolution of the FWHM of the stimulated band as a function of pressure. The broadening of the stimulated band is likely

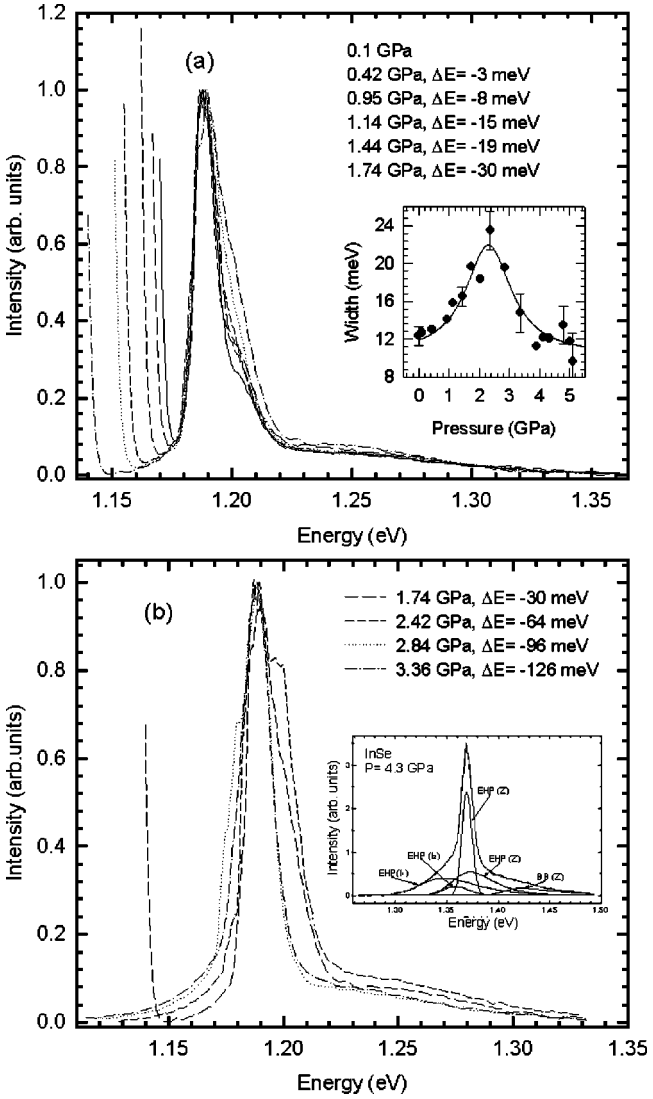

FIG. 10. Room-temperature HDPL spectra of InSe at different pressures under the same high-density excitation conditions. Spectra have been normalized with respect to the maximum of the DEHP band and shifted in energy by ΔE in order to compare the shape of the spectrum at different pressures. (a) Spectra from 0 to 1.74 GPa; (b) spectra from 1.74 to 3.36 GPa. Inset of (a): pressure dependence of the width of the stimulated DEHP band as a function of pressure. Inset of (b): example of the decomposition of the HDPL spectrum at 4.3 GPa.

due to the transfer of the excitation between two modes of the sample cavity and the coexistence of both modes in a given pressure range. This explanation is supported by the fact that the separation of the two apparent stimulated peaks is of the same order than the separation between the interference fringe maxima of the transmittancy spectrum.

A deep knowledge of the EHP can be obtained from the fit of the EHP emission profiles. The EHP is a degenerate system of high-density electrons and holes whose spontaneous radiative recombination profile is given by the convolution of the occupied density of states of electrons and holes[56]

$$I(\hbar\omega) = A\int_0^{\hbar\omega - E_{\text{onset}}} D_e(E)D_h(\hbar\omega - E_{\text{onset}} - E) \times f_e(E,\varepsilon_e,T)f_h(\hbar\omega - E_{\text{onset}} - E,\varepsilon_h,T)dE, \quad (9)$$

where the factor A contains the transition matrix element, D_e, ε_e, and D_h, ε_h are the electron and hole density of states and quasi-Fermi levels, and f_e and f_h are the Fermi functions for electrons and holes, $\hbar\omega$ is the emitted photon energy and E_{onset} is the energy of the onset of the EHP luminescence. In the case of radiative recombination from the direct gap, $E_{\text{onset}}=E_{\text{RG}}$, with E_{RG} the renormalized direct gap due to the Coulombian interaction between electrons and holes; and the joint density of states in Eq. (9) is proportional to the squared root of the energy, $(\hbar\omega\text{-}E_{\text{onset}})^{1/2}$. In the case of radiative recombination from the indirect gap, $E_{\text{onset}}=E_{\text{RG}}-\hbar\omega_f$, with $\hbar\omega_f$ the energy of the emitted phonon because the probability of the recombination process with phonon absorption is negligible;[57] and the joint density of states in Eq. (9) is proportional to the square of the energy, $(\hbar\omega-E_{\text{onset}})^2$. The stimulated radiative recombination of an electron-hole plasma is also given by Eq. (9), but the factor $f_e\cdot f_h$ must be replaced by the factor $(1-f_e-f_h)$.[51] As an example, the inset of Fig. 10(b) shows the HDPL spectrum of InSe at 4.3 GPa and its decomposition in spontaneous and stimulated bands. The two bands named as EHP(Z) correspond to the stimulated (high intensity) and spontaneous (low intensity) emission bands of the direct electron-hole plasma. The two bands named as EHP(I_1) and EHP(I_2) correspond to the spontaneous emission bands of the I_1 and I_2 indirect electron-hole plasmas, respectively. The band named BB is the same observed in low-density excitation measurements.

Since low-energy tails of spontaneous emission bands from indirect gaps should exhibit a quadratic dependence

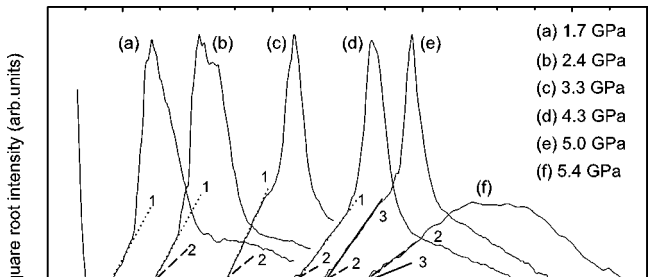

FIG. 11. HDPL spectra in InSe at room temperature as a function of pressure. The square root of the PL intensity vs the photon energy is represented in order to observe the EHP emission coming from indirect transitions. A stimulated emission peak dominates the spectra. A straight line (dotted line 1) can be extrapolated from the low-energy tail of the HDPL spectra up to 1.7 GPa. A new straight line (dashed line 2) with a different slope and a different pressure coefficient can be extrapolated above this pressure. A third line (solid line 3) also with a different pressure coefficient can be extrapolated from 4.3 GPa upwards. The first straight line is no longer seen above 4.3 GPa.

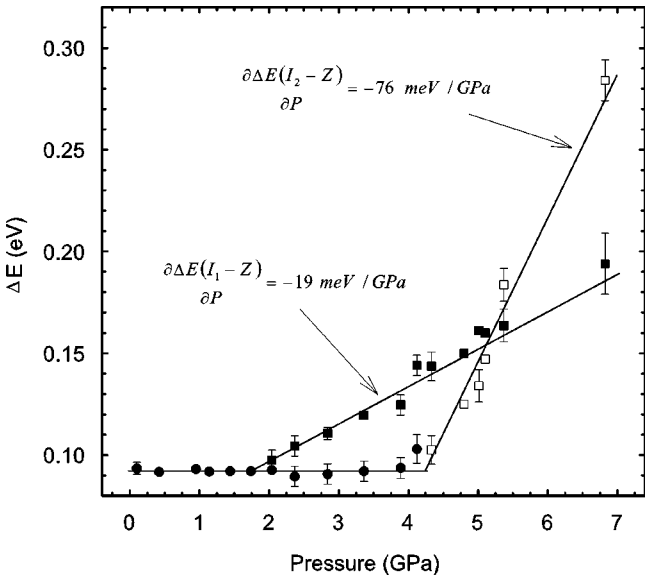

FIG. 12. Evolution of the energy separation between the energy of the zero-intensity extrapolation of lines 1, 2, and 3 and the direct band gap at Z as a function of pressure. Solid circles, solid squares, and hollow squares correspond to the separation between the low-energy tail of lines 1, 2, and 3 and the direct band gap, respectively. Solid lines indicate the pressure coefficients estimated for the direct-to-indirect band-gap separations.

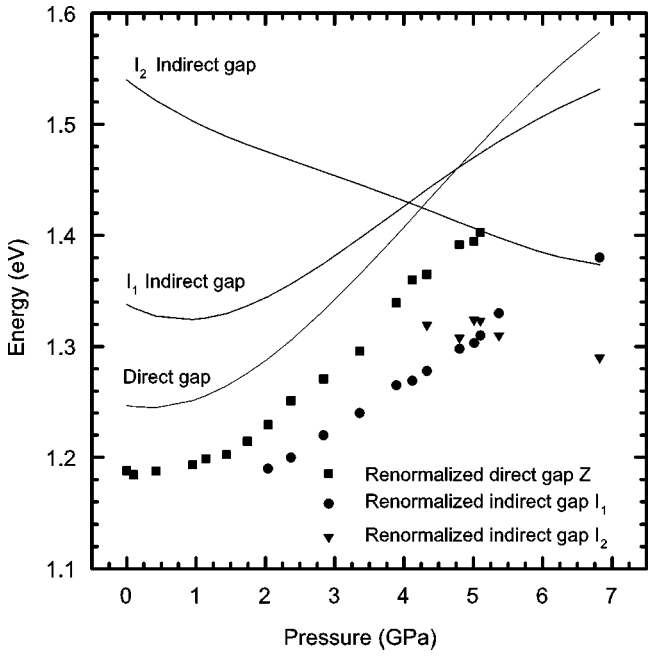

FIG. 13. Evolution of the energies of the renormalized band gaps as a function of pressure (symbols). The renormalized direct band-gap energy (dotted squares) has been obtained from the fit of the DEHP stimulated emission band to Eq. (9). The renormalized indirect gaps I_1 and I_2 minus a phonon (circles and triangles, respectively) have been obtained from the extrapolation to zero intensity of the straight lines 2 and 3 in Fig. 11. The band-gap pressure dependencies obtained from absorption measurements (Ref. 34) (solid lines) are also shown for comparison.

with photon energy, in Fig. 11 we plotted the squared root intensity of the HDPL spectra as a function of the photon energy for different pressures in order to discriminate between the different straight lines corresponding to possible indirect transitions in our spectra. Several straight lines can be observed at the low-energy tail of the spectra at different pressures. We identify the different lines on the basis of the different pressure coefficients of their extrapolations to zero intensity. Below 1.7 GPa only one low-energy straight line (dotted line 1 in Fig. 11) is observed, showing the same energy shift as the stimulated DEHP and spontaneous BB bands. Above 1.7 GPa, we observe a second low-energy straight line (dashed line 2 in Fig. 11). This second line extrapolates at a lower energy than that of the previous line and shows a smaller positive pressure coefficient than the direct gap of InSe. The coexistence of these two lines can be observed up to a pressure of 4.3 GPa. Above this pressure, two different straight lines could also be observed. One of them exhibits the same pressure coefficient as line 2, but the other one (solid line 3 in Fig. 11) exhibits a negative pressure coefficient.

The nature of lines 1, 2, and 3 can be reasonably deduced on the basis of their pressure coefficients and the detailed knowledge of the electronic band structure. We assign line 1 to the direct gap and this line can be interpreted as due to the Lorentzian carrier collision broadening of the spontaneous DEHP emission.[55,58–60] Its disappearance above 4.3 GPa clearly correlates to the decrease of the stimulated emission. We assign lines 2 and 3 to the low-energy tails of spontaneous emission bands from indirect electron-hole plasmas (IEHP). These plasmas can certainly exist at low pressures but are more clearly observed above 1.7 and 4.3 GPa, respectively, due to the pressure-induced direct-to-indirect crossovers. Line 2 would correspond to the spontaneous indirect radiative recombination of electrons thermalized to the CBM at Z and holes thermalized at the donut-like VBM (I_1 indirect gap in Fig. 2). Line 3 would correspond to the spontaneous indirect radiative recombination of electrons thermalized to the CBM at A and holes thermalized to the VBM at Z (I_2 indirect gap in Fig. 2).

Figure 12 shows the energy difference between the direct energy emission and the energy of the zero-intensity extrapolated lines 1, 2, and 3 in Fig. 11 as a function of pressure. As expected, the energy difference between the direct gap (BB emission) and line 1 is independent of pressure (see solid circles in Fig. 12). This result confirms the previous assignment of line 1 to the Lorentzian broadening of the stimulated DEHP emission. On the other hand, the energy difference between the direct gap and lines 2 and 3 (solid and blank squares in Fig. 12, respectively) depends on pressure and exhibits pressure coefficients of -19 ± 5 and -76 ± 10 meV/GPa, respectively. These pressure coefficients are similar to those observed for the I_1-Z and $Z-I_2$ indirect gaps in absorption measurements under pressure (with respect to the Z direct absorption edge).[34] This result supports the previous assignment of lines 2 and 3 to indirect emissions.

Figure 13 shows a comparison of the band-gap pressure dependencies obtained from HDPL with those obtained from absorption measurements.[34] Symbols in Fig. 13 correspond to the energies of the renormalized band gaps as obtained from HDPL measurements. The renormalized direct band-gap energy (dotted squares) has been obtained from the fit of the DEHP stimulated emission band to Eq. (9). The renormalized indirect gaps I_1 and I_2 minus a phonon have been obtained from the extrapolation to zero intensity of the straight lines 2 and 3 in Fig. 11, which correspond to the low-energy tails of the IEHP spontaneous emission bands, respectively. Solid lines in Fig. 13 correspond to the pressure dependence of the direct band gap at Z and the indirect band gaps I_1-Z and $Z-I_2$, respectively, as obtained from absorption experiments.[34]

The energy difference between the corresponding lines and symbols allows for an estimation of the renormalization energy of each band gap at the average photoexcited electron density used in the experiment under pressure (around 6×10^{19} cm^{-3}). This value is reasonable if we consider the reduction of the excitation intensity due to laser reflection in the diamond anvils and the increased weight of surface recombination in samples introduced in the DAC. In this sense, surface defects are expected by plastic deformation of micrometer-size samples after its manipulation to fit them into the DAC. The Z direct band-gap renormalization at ambient pressure is about -60 ± 10 meV and decreases slightly with increasing pressure up to 4.3 GPa. This decrease is understood on the light of the decrease of holes thermalized to the VBM at Z with increasing pressure. The energy difference between line and symbols for the I_1 indirect band gap remains almost constant (about -140 ± 15 meV) above 1.7 GPa. Taking into account that the solid line of the indirect gap I_1 obtained from absorption measurements represents the I_1 indirect band gap plus a phonon and that solid circles represent the renormalized I_1 indirect band gap minus a phonon, and assuming that the phonon energy is around 25 meV, we can estimate the renormalization energy of the I_1 indirect bandgap to be around -90 ± 25 meV. Both the slight decrease of the direct bandgap renormalization and the constant renormalization of the I_1 indirect bandgap is consistent with the hole concentration at the Z and the donut-like VBM and the corresponding renormalization band-gap energies obtained by applying the BGRMS theory at 2 GPa in the same way as at ambient pressure in Figs. 7 and 8. On the other hand, the energy difference between the line and symbols for the I_2 indirect band gap remains almost constant (about -100 ± 15 meV) above 4.3 GPa. With the same considerations done before for the I_1 indirect band gap, and assuming a phonon energy of the same order, we can estimate the renormalization energy of the I_2 indirect band gap to be around -50 ± 25 meV. This renormalization is also consistent with the renormalization band-gap energy obtained by applying the BGRMS theory at 5 GPa in the same way we did at ambient pressure in Figs. 7 and 8.

Finally, we would like to note that our assignment for lines 1, 2 and 3 to the direct gap at Z and the I_1 and I_2 indirect gaps respectively is further supported by the fact that the intensity of the stimulated DEHP line is barely affected by the I_1-Z crossover, but strongly affected by the $Z-I_2$ crossover. This phenomenon is similar to the reversible decrease of the intensity of the direct BB band above 4 GPa in LDPL measurements of InSe already commented in Sec. III A. Furthermore, on the same basis it is reasonable to attribute the quenching of the direct emissions in HDPL measurements to the trapping of carriers thermalized in the B minima of the conduction band after the $Z-B$ crossover due to the presence of a deep trap associated to the B minima of the conduction band.[50] This trap deepens into the band gap as pressure increases thus creating a nonradiative recombination channel that is more effective than direct radiative recombination. The fact that the quenching of the DEHP stimulated emission is observed in the same pressure range for both low and high-density excitation conditions indicates that the $Z-I_2$ direct-to-indirect gap crossover occurs in both cases in this pressure range (around 4 GPa). This result is coherent with the fact that the renormalization energies for the direct and I_2 indirect gaps are practically the same within the experimental error. On the opposite, the observation of the I_1 IEHP spontaneous emission at photon energies below the stimulated emission indicates that the I_1-Z direct-to-indirect gap crossover occurs at lower pressure in high-density conditions. This result is coherent with the higher renormalization energy of the I_1 indirect gap.

IV. CONCLUSIONS

The direct-to-indirect gap crossovers observed through the pressure evolution of the line shape and intensity of LDPL spectra are in agreement with those described in Ref. 34.

The renormalization band-gap energies and direct-to-indirect gap crossover pressures, as measured in HDPL experiments under pressure agree with calculations based on the BGRMS theory and can be accounted for with the inclusion in the calculations of a donut-like maximum of the valence band near the maximum at Z.

Consequently, the information about the InSe electronic band structure provided by the present LDPL and HDPL measurements agrees with the image obtained by recent pseudopotentials and LMTO calculations,[31,33] NAO-DFT calculations[34,36] and quasi-particle GW calculations,[37] and supports previous analysis of the optical absorption coefficient of InSe and $In_{1-x}Ga_xSe$ ($x<0.2$).[34]

Therefore, we propose the following model for the band structure of InSe. At ambient pressure, the conduction band of InSe has a minimum at Z located some 300 meV below the B and the A minima, whereas the valence band has a maximum at Z located some 70 meV above a thoroidal maximum around Z. With the increase of pressure, the thoroidal maximum of the valence band becomes the absolute maximum and the minimum at B (or A) becomes the absolute minimum of the conduction band. Both band-gap crossovers occur near 4 GPa, but the valence band crossover manifests at a lower pressure in absorption and photoluminescence measurements because the excitonic crossover occurs at a lower pressure for the valence than for the conduction band and because the renormalization energy is much greater for the donut-like VBM than for the CBM at B (or A).

ACKNOWLEDGMENTS

F.J.M. acknowledges support from Generalitat Valenciana. Part of this work was supported by DGES-Spain (Project No. BFM2003-03372-C03) and Generalitat de Catalunya (No. 2001SGR333). The computations described in this work were carried out using the resources of CESCA and CEPBA coordinated by C4. G.T. acknowledges support from Ministerio de Ciencia y Tecnología of Spain.

*Author to whom correspondence should be addressed. FAX: + 34 96 652 84 25. Electronic address: fjmanjon@fis.upv.es

[1] W. Chen, J. Burie, and D. Boucher, Laser Phys. **10**, 521 (2000).
[2] A. C. Wright, T. L. Ng, and N. Maung, Adv. Mater. **12**, 273 (2000).
[3] N. B. Singh, D. R. Suhre, W. Rosch, R. Meyer, N. C. Fernelius, F. K. Hopkins, D. E. Zelmon, and R. Nayaranan, J. Cryst. Growth **199**, 588 (1999).
[4] Ch. Ferrer-Roca, J. Bouvier, A. Segura, M. V. Andrés, and V. Muñoz, J. Appl. Phys. **85**, 3780 (1999), and references therein.
[5] A. Segura, J. Bouvier, M. V. Andres, F. J. Manjón, and V. Muñoz, Phys. Rev. B **56**, 4075 (1997), and references therein.
[6] O. Lang, R. Rudolph, A. Klein, C. Pettenkofer, W. Jaegermann, J. Sánchez, A. Segura, and A. Chevy, *Photovoltaic Solar Energy Conference* (Reidel, Dordrecht, 1996), p. 2023.
[7] N. Romeo, J. Appl. Phys. **42**, 3643 (1971).
[8] P. Gomes da Costa, M. Balkanski, and R. F. Wallis, Phys. Rev. B **43**, 7066 (1991).
[9] J. F. Sánchez-Royo, A. Segura, O. Lang, C. Pettenkoffer, W. Jaegermann, A. Chevy, and L. Roa, Thin Solid Films **307**, 283 (1997).
[10] A. Koma, Thin Solid Films **216**, 72 (1992).
[11] W. Jaegermann, in *Photoelectrochemistry and Photovoltaics of Layered Semiconductors*, edited by A. Aruchami (Kluwer, Dordrecht, 1984).
[12] D. R. T. Zhan, T. U. Kampen, S. Hohenecker, and W. Braun, Vacuum **57**, 139 (2000).
[13] N. Okamoto and H. Tanaka, Mater. Sci. Semicond. Process. **2**, 13 (1999).
[14] A. A. Homs and B. Marí, J. Appl. Phys. **88**, 4654 (2000), and references therein.
[15] A. Zubiaga, J. A. García, F. Plazaola, V. Muñoz-Sanjosé, and C. Martínez-Tomás, Phys. Rev. B **68**, 245202 (2003).
[16] M. O. Godzaev and B. E. Sernelius, Phys. Rev. B **33**, 8568 (1986).
[17] R. E. Nahory, K. L Shaklee, R. F. Leheny, and J. C. De Winter, Solid State Commun. **9**, 1107 (1971).
[18] N. Kuroda, T. Nakanomyo, and Y. Nishina, Jpn. J. Appl. Phys., Suppl. **43** Suppl., 63 (1974).
[19] A. Mercier and J. P. Voitchovsky, Phys. Rev. B **12**, 2243 (1975).
[20] N. Kuroda and Y. Nishina, J. Lumin. **12/13**, 623 (1976).
[21] T. Ugumori, K. Masuda, and S. Namba, Nuovo Cimento Soc. Ital. Fis., B **38B**, 596 (1977).
[22] G. B. Abdullaev, G. L. Belenkii, E. Yu. Salaev, and R. A. Suleimanov, Nuovo Cimento Soc. Ital. Fis., B **38B**, 469 (1977).
[23] R. Baltramiejunas, V. Narkevidius, E. Skaistis, J. Vaitkus, and J. Viscakas, Nuovo Cimento Soc. Ital. Fis., B **38B**, 603 (1977).
[24] A. Cingolani, M. Ferrara, and M. Lugarà, Opt. Commun. **32**, 109 (1980).
[25] R. A. Muribeca and E. A. Meneses, Solid State Commun. **37**, 475 (1980).
[26] A. Cingolani, M. Ferrara, M. Lugarà, and F. Levy, Physica B & C **105B**, 40 (1981).
[27] A. Cingolani, M. Ferrara, M. Lugarà, and F. Lévy, Phys. Rev. B **25**, 1174 (1982).
[28] S. S. Yao and R. R. Alfano, Phys. Rev. B **27**, 2439 (1983).
[29] A. Cingolani, M. Ferrara, and M. Lugarà, Phys. Rev. B **36**, 9589 (1987).
[30] V. S. Dneprovskii, A. I. Furtichev, V. I. Klimov, E. V. Nazvanova, D. K. Okorokov, and U. V. Vandishev, Phys. Status Solidi B **146**, 341 (1988).
[31] P. Gomes da Costa, R. G. Dandrea, R. F. Wallis, and M. Balkanski, Phys. Rev. B **48**, 14 135 (1993).
[32] C. Ulrich, A. R. Goñi, K. Syassen, O. Jepsen, A. Cantarero, and V. Muñoz, *Proceedings of the 15th AIRAPT and 33 EHPRG Conference, Warsaw, Poland, 1995*, edited by W. A. Trzeciakowski (World Scientific, Singapore, 1996), p. 647.
[33] C. Ulrich, D. Olguin, A. Cantarero, A. R. Goñi, K. Syassen, and A. Chevy, Phys. Status Solidi B **221**, 777 (2000).
[34] F. J. Manjón, D. Errandonea, A. Segura, V. Muñoz, G. Tobías, P. Ordejón, and E. Canadell, Phys. Rev. B **63**, 125330 (2001).
[35] J. F. Sánchez-Royo, J. Pellicer-Porres, A. Segura, V. Muñoz-Sanjosé, G. Tobías, P. Ordejón E. Canadell, and Y. Huttel, Phys. Rev. B **65**, 115201 (2002).
[36] A. Segura, F. J. Manjón, D. Errandonea, J. Pellicer-Porres, V. Muñoz, G. Tobías, P. Ordejón, E. Canadell, D. Sánchez-Portal, and A. San Miguel, Phys. Status Solidi B **235**, 267 (2003).
[37] G. Ferlat, H. Xu, V. Timoshevskii, and X. Blase, Phys. Rev. B **66**, 085210 (2002).
[38] D. Olguin, A. Cantarero, C. Ulrich, and K. Syassen, Phys. Status Solidi B **235**, 456 (2003).
[39] H. Kalt and M. Rinker, Phys. Rev. B **45**, 1139 (1992).
[40] H. Kalt, *Optical Properties of III-V Semiconductors* (Springer, Berlin, 1996).
[41] D. Errandonea, F. J. Manjón, J. Pellicer, A. Segura, and V. Muñoz, Phys. Status Solidi B **211**, 33 (1999).
[42] F. J. Manjón, A. Segura, and V. Muñoz, High Press. Res. **18**, 81 (2000).
[43] A. Chevy, J. Cryst. Growth **67**, 119 (1984).
[44] R. Le Toullec, J. P. Pinceaux, and P. Loubeyre, High Press. Res. **1**, 77 (1988).
[45] G. J. Piermarini, S. Block, and J. D. Barnett, J. Appl. Phys. **44**, 5377 (1973).
[46] G. J. Piermarini, S. Block, J. D. Barnett, and R. A. Forman, J. Appl. Phys. **46**, 2774 (1975).
[47] N. Piccioli, R. Le Toullec, F. Bertrand, and J. C. Chervin, J. Phys. (Paris) **42**, 1129 (1981).
[48] A. R. Goñi, A. Cantarero, U. Schwarz, K. Syassen, and A. Chevy, Phys. Rev. B **45**, 4221 (1992).
[49] K. V. Shalímova, *Semiconductor Physics* (Mir, Moscow, 1975),

p. 189.
[50] D. Errandonea, A. Segura, J. F. Sánchez-Royo, V. Muñoz, P. Grima, A. Chevy, and C. Ulrich, Phys. Rev. B **55**, 16 217 (1997).
[51] C. F. Klingshirn, *Semiconductor Optics* (Springer, Berlin, 1997).
[52] P. Vashista and R. K. Kalia, Phys. Rev. B **25**, 6492 (1982).
[53] W. F. Brinkmann and T. M. Rice, Phys. Rev. B **7**, 1508 (1973).
[54] Ch. Ferrer–Roca, A. Segura, M. V. Andrés, J. Pellicer, and V. Muñoz, Phys. Rev. B **55**, 6981 (1997).
[55] H. Haug and D. B. Tran Thoai, Phys. Status Solidi B **98**, 581 (1980).
[56] Ya. Pokrovskii, Phys. Status Solidi A **11**, 385 (1972).
[57] W. P. Dumke, Phys. Rev. **127**, 1559 (1962).
[58] M. Capizzi, S. Modesti, A. Frova, J. L. Staehli, M. Guzzi, and R. A. Loan, Phys. Rev. B **29**, 2028 (1984).
[59] Lorentzian profile always may be developed into a series of parabolic terms in a given energy range. This is the reason why the Lorentzian low-energy tail of the spontaneous DEHP band may be observed as a straight line in the spectra of the square root PL intensity as function of photon energy.
[60] P. T. Landsberg, Phys. Status Solidi **15**, 623 (1966).